## Title
In situ raman study of nickel oxide and gold-supported nickel oxide catalysts for the electrochemical evolution of oxygen



## Journal
Journal of Physical Chemistry C, 116(15)

## ISSN
1932-7447

## Authors
Yeo, BS
Bell, AT

## Publication Date
2012-04-19

## DOI
10.1021/jp3007415

Peer reviewed

# In Situ Raman Study of Nickel Oxide and Gold-Supported Nickel Oxide Catalysts for the Electrochemical Evolution of Oxygen

Boon Siang Yeo and Alexis T. Bell*

Chemical Sciences Division, Lawrence Berkeley National Laboratory, 1 Cyclotron Road, Berkeley, California 94720, United States, and Department of Chemical and Biomolecular Engineering, University of California Berkeley, Berkeley, California 94720-1462, United States

* *Supporting Information*

ABSTRACT: An in situ Raman spectroscopic investigation has been carried out to identify the composition of the active phase present on the surface of nickel electrodes used for the electrochemical evolution of oxygen. The electrolyte in all cases was 0.1 M KOH. A freshly polished Ni electrode oxidized upon immersion in the electrolyte and at potentials approaching the evolution of oxygen developed a layer of γ-NiOOH. Electrochemical cycling of this film transformed it into β-NiOOH, which was observed to be three times more active than γ-NiOOH. The higher activity of β-NiOOH is attributed to an unidentified Ni oxide formed at a potential above 0.52 V (vs Hg/HgO reference). We have also observed that a submonolayer of Ni oxide deposited on Au exhibits a turnover frequency (TOF) for oxygen evolution that is an order of magnitude higher than that for a freshly prepared γ-NiOOH surface and more than 2-fold higher than that for a β-NiOOH surface. By contrast, a similar film deposited on Pd exhibits a TOF that is similar to that of bulk γ-NiOOH. It is proposed that the high activity of submonolayer deposits of Ni oxide on Au is due to charge transfer from the oxide to the highly electronegative Au, leading to the possible formation of a mixed Ni/Au surface oxide.

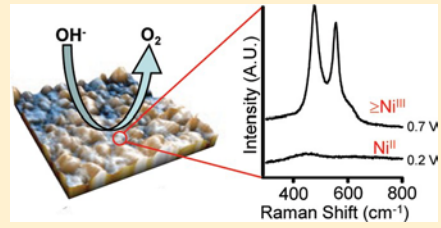


## 1. INTRODUCTION

A sustainable supply of hydrogen for various applications (e.g., fuel cells and removal of oxygen from biomass) can be achieved by the efficient electrochemical splitting of water.[1,2] This process consists of two parts: the cathodic hydrogen evolution reaction (HER, $2H^+ + 2e \rightarrow H_2$) and the anodic oxygen evolution reaction (OER, $4OH^- \rightarrow 2H_2O + 4e + O_2$). However, even with the most active electrocatalysts available, ruthenium and iridium oxides, the potential required to split water is substantially greater than the thermodynamic value of 1.23 V (vs RHE), due primarily to the high overpotential associated with the OER. Since ruthenium and iridium are not earth-abundant and are hence expensive, cheaper but less efficient catalysts such as nickel and its alloys are used in commercial alkaline electrolyzers.[3−5]

The activity of Ni electrocatalysts for OER is known to differ by more than an order of magnitude depending on the manner of electrode preparation.[6−8] Previous work has shown that $O_2$ evolution occurs on oxidized surfaces and that the composition of the surface depends on the electrolyte pH.[7,9−11] When a nickel metal electrode is immersed in an alkaline solution such as 0.1 M KOH, hydrous α-$Ni(OH)_2$ is formed spontaneously on its surface. This hydroxide layer can be aged in base or in vacuum to give anhydrous β-$Ni(OH)_2$.[12] If the working potential is increased above 450 mV (vs Hg/HgO reference), α-$Ni(OH)_2$ and β-$Ni(OH)_2$ oxidize to γ-NiOOH and β-NiOOH, respectively. These two processes are termed α/γ and β/β, respectively. β-NiOOH can also be converted to γ-NiOOH above 600 mV, which is below the potential for the electrochemical evolution of $O_2$ (>650 mV).

Ni β/β electrodes exhibit higher water oxidation activity than Ni α/γ electrodes.[6−8] The reason for the apparent higher activity of β-NiOOH versus γ-NiOOH, and whether the former is even the true catalytic material, has been a subject of controversy. While the oxidation states of Ni in $Ni(OH)_2$, $Ni(OH)_2$, and β-NiOOH are +2, +2, and +3, respectively, it has been reported that 1.67 electrons are required to oxidize α-$Ni(OH)_2$ to γ-NiOOH, suggesting that γ-NiOOH may contain $Ni^{IV}$ cations.[13] Consistent with this view and with thermodynamics, Ni has been proposed to oxidize to γ-NiOOH during OER, with $Ni^{IV}$ peroxide ($NiOO_2$) as an intermediate to $O_2$ formation.[11] It is notable, though, that both ex situ X-ray photoelectron spectroscopy (XPS) and in situ X-ray absorption fine structure spectroscopy of γ-NiOOH show only the presence of $Ni^{III}$ cations.[14,15] Thus, to date, there is no conclusive data indicating that $Ni^{IV}$ is better than $Ni^{III}$ for catalyzing the OER.

We have recently demonstrated that the turnover frequency (TOF) for $O_2$ evolution exhibited by ~0.4 ML of cobalt oxide deposited on a Au substrate is forty times higher than that of bulk Co oxide.[16] The observed high activity was attributed to Au-mediated oxidation of the Co oxide films to give $Co^{IV}$ species, which are believed to be catalytically active for OER.

Our proposition is supported by other studies, which suggest that high valent metal cations such as $Ru^{V}$ or $Fe^{VI}$ are the active sites for catalyzing OER.[17,18] These studies also propose that hydroperoxy (OOH) species are the key intermediates in the OER. Thus, the likely role of the highly oxidized metal cations is to facilitate OOH formation and/or conversion to $O_2$. Hydroperoxy species have also been proposed as critical intermediates in the evolution of $O_2$ from oxidized Ni.[17] On the basis of these observations, it is reasonable to expect that thin layers of Ni oxide supported on Au would be more active for OER than bulk Ni.

We report here the first in situ Raman investigation of the composition of bulk Ni catalysts and thin layers of Ni hydroxide deposited on Au at potentials relevant for the electrochemical oxidation of water. We have observed that the type of NiOOH formed on bulk Ni electrodes depends on the method of electrode pretreatment. We also found that a submonolayer of Ni oxide deposited on Au has an order of magnitude higher OER activity compared to a freshly prepared Ni α/γ surface, and more than twice that for a Ni β/β surface. Electronic charge transfer from Ni oxide to Au is envisaged to be responsible for the higher activity of the former.

## 2. EXPERIMENTAL SECTION

**2.1. Apparatus for in Situ Raman Spectroscopy and Electrochemistry.** A specially built Teflon cell was used for the combined electrochemical and in situ Raman spectroscopy studies.[16] This cell contains a Au, Ni, or Pd circular working electrode with a geometric surface area of 0.785 $cm^2$. A Pt wire and Hg/HgO (CH instruments) electrode served as the counter and reference electrodes, respectively. Current−voltage curves were generated using a galvanostat/potentiostat (Gamry 600). In situ Raman spectra of the electrodes were recorded using a confocal Raman microscope (LabRam HR, Horiba Jobin Yvon). Spectra were acquired with 1−2 mW of 633 nm laser excitation at the sample surface. A high numerical aperture water-immersion objective (N.A. = 1.23, LOMO) was used in order to achieve a high efficiency in the collection of the Raman scattered radiation. The acquisition times for surface-enhanced (with roughened Au as substrate) and normal Raman spectra were 3−5 and 15 s, respectively.

Prior to investigation, the Au, Ni, and Pd anodes were polished mechanically with micrometer-sized alumina powders and then sonicated briefly in 1 M KOH solution and $H_2O$. Upon immersion of the Ni electrode into the alkaline electrolyte, a layer of α-$Ni(OH)_2$ is formed spontaneously on its surface even in the absence of an applied potential.[7,8] A β-$Ni(OH)_2$ layer on the Ni electrode was prepared by cycling the initially formed α-$Ni(OH)_2$ layer from 0.25 to 0.53 V (vs Hg/HgO) in 8 M KOH at 0.1 mV/s for at least 15 h.[12] A Pt pseudo reference was used in this preparation ($E_{\text{Pt pseudo reference}} = E_{\text{Hg/HgO}} - 0.5$ V). The formation of β-$Ni(OH)_2$ is commonly thought to occur via the dehydration and ordering of an α-$Ni(OH)_2$ layer.[19] However, an anion-exchange mechanism, i.e., interlamellar replacement of $NO_3^-$ by $OH^-$ from the KOH solution, has also been proposed.

The Au electrode was roughened electrochemically.[20] α-$Ni(OH)_2$ with thicknesses from 0.14−64 ML (ML = monolayer equivalent) was deposited galvanostatically onto the Au or Pd electrode from a 0.01 M $Ni(NO_3)_2$ solution (pH 5.61, prepared from nickel nitrate hexahydrate, Aldrich, 99.999%) using 0.1−45 mC cathodic charges (current = −10 μA).[21,22] This process can be written as

$$NO_3^- + 7H_2O + 8e \rightarrow NH_4^+ + 10OH^-$$

$$Ni^{2+} + 2OH^- \rightarrow Ni(OH)_2$$

The Faradaic deposition efficiency was estimated by integrating the Ni oxide reduction peak in the various cyclic voltammograms.[21] A value of not more than ∼67% was obtained regardless of the film thickness, which agrees closely with the value of 68% reported by Kostecki and McLarnon using a similar setup.[22]

**2.2. Reagents and Experimental Procedure.** Ultrapure type 1 $H_2O$ (Millipore) was used to prepare solutions and to wash electrodes. The solutions were deoxygenated with $N_2$ gas before each experiment. Electrolyte 0.1 M KOH (prepared from GR ACS grade solid KOH, EMD Chemicals) was used for the OER study. When possible, the current densities were evaluated using the true surface area, as determined by the double layer capacitance method (for bulk Ni and thick Ni oxide films on Au) or integration of oxide reduction peaks (for bulk Au and Pd) (section S1 of Supporting Information). Since there is no suitable method to measure the surface area of very thin Ni oxide films (<1 ML) on Au, we used the true surface area of the Au substrate. The true surface area of each sample was used in determining its current density and TOF. This protocol ensures that the calculated activity of the electrodes is not affected by current fluctuations arising from differences in surface area. *iR*-compensation was made during the electrochemical measurements using the current interrupt mode. Prior to recording electrochemical OER data with the Ni or Ni oxide coated electrodes, cyclic voltammetry (CV) or linear sweep voltammetry (LSV) sweeps were made from 0 to 0.8 V until the surface of the electrodes were stabilized (section S2 of Supporting Information). All the linear sweep voltammograms presented in this work were collected from 0 to 0.8 V at 1 mV/s. The experiments were performed at a room temperature of 295 K. Unless otherwise mentioned, all potentials cited in this work are referenced to the Hg/HgO electrode.

## 3. RESULTS AND DISCUSSION

**3.1. Characterization of Ni α/γ and Ni β/β Electrodes during Electrochemical Oxygen Evolution.** Cyclic and linear sweep voltammograms for the Ni α/γ and Ni β/β electrodes in 0.1 M KOH are presented in Figure 1a,b. α-$Ni(OH)_2$ is oxidized to γ-NiOOH at a lower potential than β-$Ni(OH)_2$ is oxidized to β-NiOOH.[22] Oxygen evolution occurs on both surfaces above 650 mV; however, the OER current for Ni β/β is higher than that for Ni α/γ. These observations are consistent with those reported previously.[7,8] To determine the intrinsic activity of the Ni surfaces, we evaluated the turnover frequency for $O_2$ evolution following the procedure described in our previous work.[16] The TOF gives the number of $O_2$ molecules formed per second per Co site, assuming that all surface Co atoms are active. At 700 mV, the TOF for Ni α/γ is 0.23 $s^{-1}$ and that for Ni β/β is 0.68 $s^{-1}$. Tafel slopes and reaction orders in $OH^-$ concentration were measured for the Ni α/γ and Ni β/β electrodes in 0.1, 0.5, and 1 M KOH (section S3 in Supporting Information). The Tafel slopes for the Ni α/γ and Ni β/β electrodes measured at ∼650 mV are ∼46 and ∼56 mV/dec, respectively, and are consistent with values reported previously.[6,17,23] The reaction orders in $OH^-$ concentration for Ni α/γ and Ni β/β are ∼0.92 and ∼0.69, respectively. The orders in $OH^-$ concentration for Ni surfaces conditioned electrochemically in several ways have been

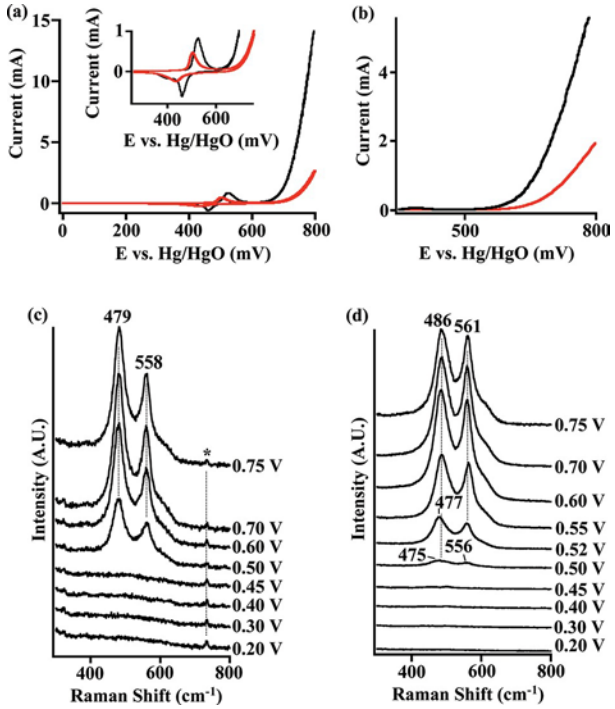


Figure 1. (a) Cyclic voltammograms and (b) linear sweep voltammograms of Ni α/γ (red trace) and Ni β/β (black trace) electrodes. In situ Raman spectra collected during linear sweep voltammetry from (c) Ni α/γ and (d) Ni β/β electrodes. The 735 $cm^{-1}$ peak in panel c originates from the Teflon film used in covering the water immersion objective.

reported to be ~1.[7] It is noted, though, that this parameter depends on the shape of the $OH^-$ adsorption isotherm, which varies with the condition of the electrode.[24]

The Raman spectra of Ni α/γ and Ni β/β electrodes recorded during an anodic LSV scan are shown in Figure 1c,d. The spectra are devoid of signals at potentials below 0.45 V where it would be expected to observe α-$Ni(OH)_2$ or β-$Ni(OH)_2$. We believe that the absence of vibrational features for α-$Ni(OH)_2$ and β-$Ni(OH)_2$ is due to the low Raman scattering cross-section for these species.[22] For the Ni α/γ electrode, peaks appear at ~479 and ~558 $cm^{-1}$ for potentials ≥0.50 V. The frequencies and relative intensities of these two bands match well with those of γ-NiOOH.[21,25] The intensities of these two features are stronger than those of α-$Ni(OH)_2$ because of resonance Raman enhancement of NiOOH.[26] For the Ni β/β electrode, broad peaks observed at 475−477 $cm^{-1}$ and ~556 $cm^{-1}$ at 0.50 V can be assigned to β-NiOOH.[25] These bands subsequently shift to 486 and 561 $cm^{-1}$ as the potential is raised to 0.75 V. The increase in frequencies with higher potentials is similar to what has been observed during the oxidation of β-$Ni(OH)_2$ deposited on a Ti/$SnO_2$ substrate.[27]

At first glance, the evolution of the Raman spectra for the Ni β/β appears to be similar to that for the Ni α/γ. However, there is a significant difference. Above 0.52 V, the ratio of intensities of the 479 $cm^{-1}$ and 558 $cm^{-1}$ bands of Ni α/γ remain constant (Figure 2a), indicating no further transformation of γ-NiOOH, consistent with predictions from the Pourbaix diagram of Ni.[9] By contrast, the 560 $cm^{-1}$ band of Ni β/β becomes more intense relative to the band at 485 $cm^{-1}$ for voltages between 0.52 to 0.75 V (Figure 2b).

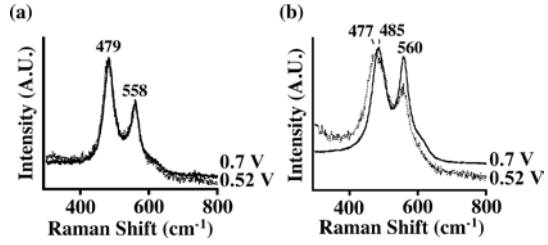


Figure 2. In situ Raman spectra of a (a) Ni α/γ and (b) Ni β/β electrode during a linear sweep voltammetry scan. The two spectra in each panel are collected at 0.7 and 0.52 V. The spectra are normalized to the ~480 $cm^{-1}$ band.

The possibility that β-NiOOH transforms to γ-NiOOH can be eliminated because the ratio of intensities of the bands at 479 $cm^{-1}$ and 558 $cm^{-1}$ seen in the spectrum of γ-NiOOH is higher than that seen in the spectrum of β-NiOOH (Figure 1c,d). Hence, if γ-NiOOH were formed, the ratio of the intensity of the 485 $cm^{-1}$ band to that of the 560 $cm^{-1}$ band should increase; however, the opposite was observed. Furthermore, repeated potential cycling of the Ni β/β electrode from 0 to 0.8 V gave reproducible CV cycles indicating no change in the chemical composition of the electrode. (section S2 in Supporting Information). These observations demonstrate that while β-NiOOH undergoes some type of transformation above 0.52 V, γ-NiOOH is not formed.

Our experiments show that an α-$Ni(OH)_2$ layer freshly formed on the surface of a bulk Ni electrode undergoes electrochemical oxidation to γ-NiOOH. Repeated cycling of a Ni α/γ electrode in 8 M KOH results in the transformation of the α-$Ni(OH)_2$ layer into a β-$Ni(OH)_2$ layer. Upon electrochemical oxidation, this film transforms to β-NiOOH, which in turn appears to convert at above ~0.52 V to another form of Ni oxide (but not γ-NiOOH). This observation is consistent with combined near normal incidence reflectance spectroelectrochemical (NNIRS) and cyclic voltammetry measurements, which indicate that a significant amount of β-NiOOH converts to an unidentified form of Ni oxide at potentials above ~0.52 V (vs Hg/HgO reference).[28] Therefore, in contrast to conventional thinking, we propose here that β-NiOOH itself may not be the actual catalyst for OER.[6−8]

**3.2. Characterization of Ni Oxide Deposited on Au and Pd Electrodes during Oxygen Evolution.** Linear sweep voltammetry was performed on Au anodes containing electrodeposited α-$Ni(OH)_2$, and representative measurements are presented in Figure 3a. Figure 3b shows a plot of the current density measured at a potential of 700 mV versus the number of monolayers of α-$Ni(OH)_2$ deposited (0.14 to 64 ML). The OER current density rises to a maximum of 0.4 mA/$cm^2$ for a 2.8 ML Ni oxide layer and then falls to 0.03 mA/$cm^2$ for thicker films. The TOFs for $O_2$ evolution for the α-$Ni(OH)_2$ deposit were also evaluated at 700 mV. Figure 3c shows that the TOF decreases rapidly as the coverage of Ni oxide on the Au electrodes increases, and then slowly approaches the value for α-$Ni(OH)_2$ formed on bulk Ni. For 0.14 ML Ni oxide deposited on Au, the TOF for oxygen evolution is ~1.9 $s^{-1}$. This is an order of magnitude higher than that for a thick (42−64 ML) layer of Ni oxide (0.09−0.17 $s^{-1}$), and more than twice that of the Ni β/β (0.68 $s^{-1}$). To further confirm that the high activity of submonolayer deposits of α-$Ni(OH)_2$ on Au is due to interaction of the deposit with Au, similar experiments were carried out in which 0.1 and 2 mC of

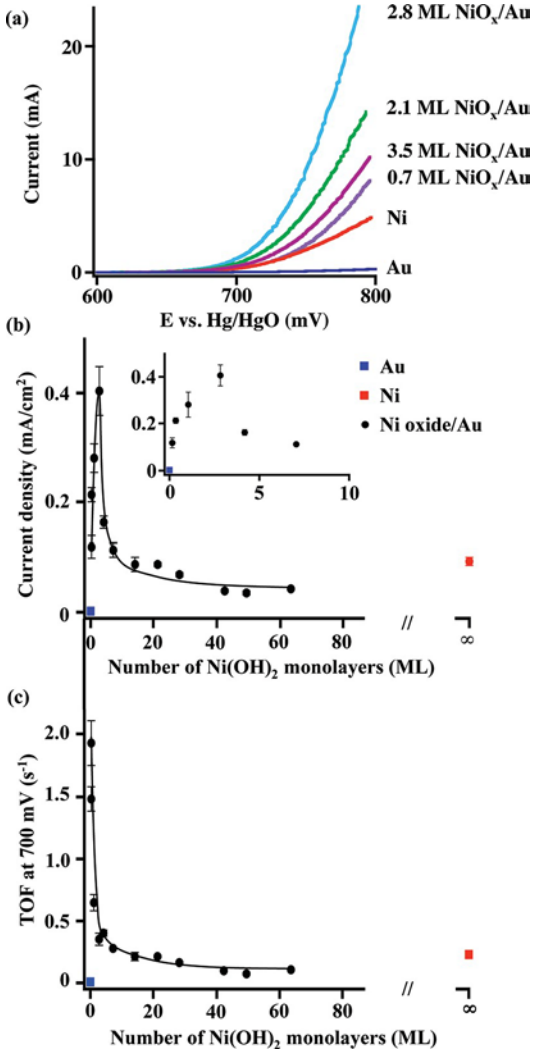


Figure 3. (a) Representative linear sweep voltammograms of Au electrodes deposited with α-Ni(OH)$_2$. The LSVs for Ni α/γ and Au are also included. The scan rate is 1 mV/s. Note that the current increases as the thickness of deposited α-Ni(OH)$_2$ increases from 0.7 to 2.8 ML but drops rapidly when thickness goes to 3.5 ML. Plots of (b) current densities and (c) turnover frequencies of Ni oxide/Au electrodes (evaluated at a potential of 700 mV) vs the number of monolayers of α-Ni(OH)$_2$ present. The insert in panel b is a blow-up of the plot from 0 to 10 ML. The data points of Ni α/γ and Au electrodes are also included.

α-Ni(OH)$_2$ were deposited on Au and Pd electrodes. Figures 4a and S4, Supporting Information, show that the measured current density for α-Ni(OH)$_2$ deposited on Au is significantly higher than that for an equivalent deposit on Pd, in agreement with similar observations reported for cobalt oxide deposited on Au verses Pd electrodes (section S4 in Supporting Information).[16] Further evidence for differences in the interactions of Ni(OH)$_2$ with Au and Pd are revealed in the cyclic voltammograms for the two systems; α-Ni(OH)$_2$/Pd clearly resembles bulk Ni more than α-Ni(OH)$_2$/Au (Figure 4b). The average TOFs for 0.1 and 2 mC α-Ni(OH)$_2$ deposited on a Au electrode are 1.93 and 0.35 s$^{-1}$, respectively. However, the same amounts of α-Ni(OH)$_2$ deposited on Pd yield TOFs of 0.20 and 0.11 s$^{-1}$, respectively. These results indicate that Pd, unlike Au, does not interact strongly with α-Ni(OH)$_2$.

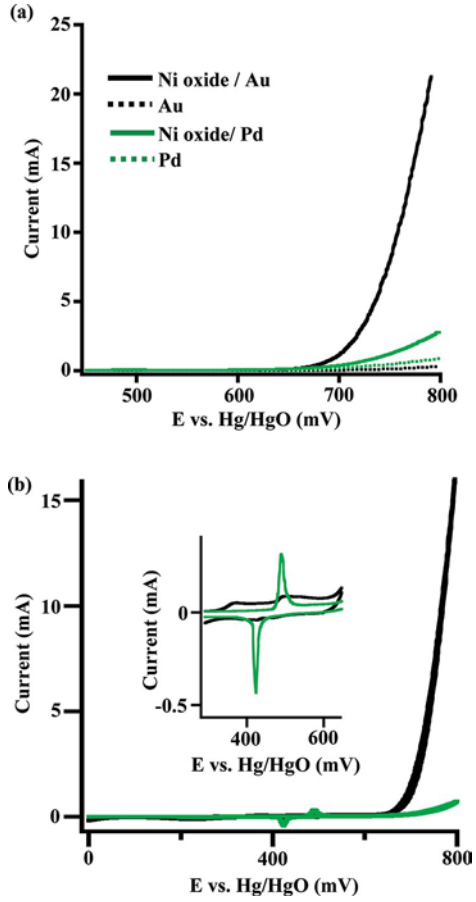


Figure 4. (a) Linear sweep and (b) cyclic voltammograms of Au and Pd electrodes deposited with 2 mC of α-Ni(OH)$_2$. The insert in panel b is a zoomed-in picture of the anodic and cathodic peaks of Ni oxide.

Figure 5 shows surface-enhanced Raman spectra acquired during linear sweep voltammetry scans from 0 to 0.8 V for a Au electrode and a Au electrode containing progressively thicker deposits of α-Ni(OH)$_2$. The spectrum of the Au electrode is featureless initially, but as the potential is raised, a single broad band appears (Figure 5a). The center of this feature occurs at 555 cm$^{-1}$ at a potential of 0.4 V and then shifts to 585 cm$^{-1}$ as the potential is raised to 0.75 V. This band is attributable to Au oxide formed via anodic oxidation of metallic Au. Its position and shift in frequency with applied potential are identical to those observed in previous studies of Au elecrodes.[20,29] The spectrum for 1.1 ML of Ni oxide deposited on Au (Figure 5b) shows a band nearly identical to that for bare Au, but its intensity is much higher at every potential. Increasing the thickness of the Ni oxide deposit to 2.8 ML produces a change in the Raman spectrum (Figure 5c). While a single broad band now centered at 552 cm$^{-1}$ is seen at 0.4 V, this peak shifts only +2−3 cm$^{-1}$ by 0.50 V. By contrast, the position of the band for pure Au oxide shifts by +10 cm$^{-1}$ to 565 cm$^{-1}$ by 0.50 V. When the potential is raised above 0.6 V, clearly defined bands are observed at 482 and 558 cm$^{-1}$. Increasing the thickness of the Ni oxide deposit to 4.2 ML results in the appearance of a pair of broad overlapping bands in the region of 400−500 cm$^{-1}$ for an applied potential of 0.2 V (Figure 5d). Raising the potential of this electrode to 0.45 V results in the appearance of a better defined peak at 555 cm$^{-1}$ and above 0.5 V in the appearance of 479 cm$^{-1}$ and 558 cm$^{-1}$ bands from γ-NiOOH. A similar pattern was observed for the sample containing a 64 ML of Ni

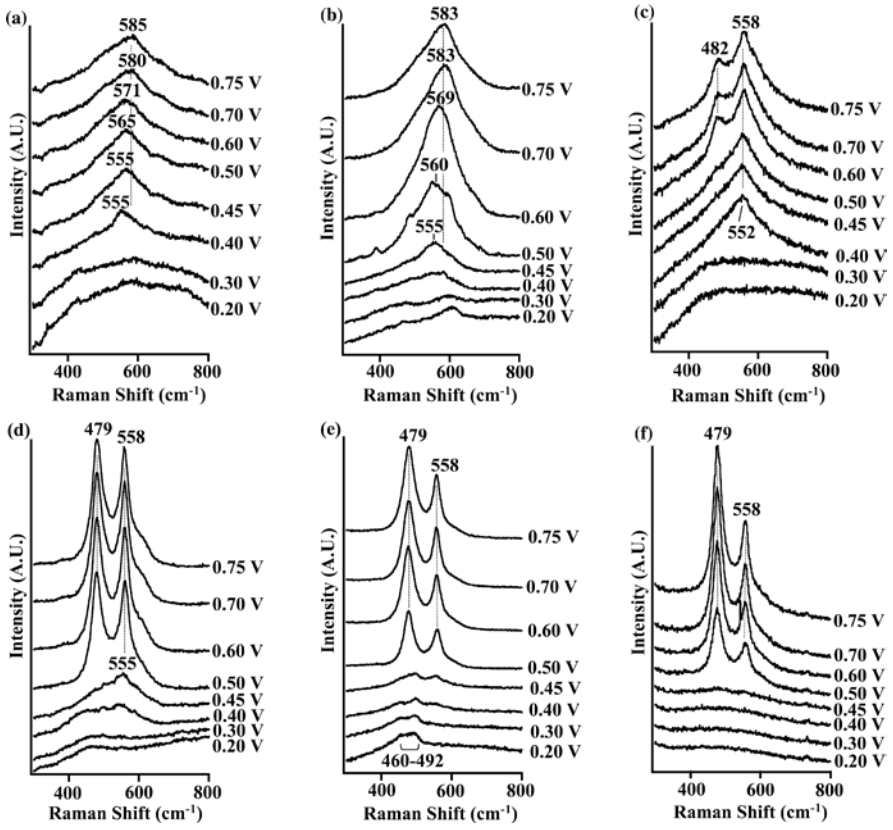


Figure 5. In situ Raman spectra collected during linear sweep voltammetry: roughened Au surface deposited with (a) 0 ML (clean), (b) ~1.1 ML, (c) ~2.8 ML, (d) ~4.2 ML, and (e) ~64 ML of α-$Ni(OH)_2$ and (f) ~2.8 ML of α-$Ni(OH)_2$ deposited on Pd; 2 mC of α-$Ni(OH)_2$ was deposited for the samples used in panels c and f.

oxide on Au (Figure 5e). The principal difference here is that the overlapping bands in the region of 460−492 $cm^{-1}$ are much sharper at 0.2 V, and the bands at 479 $cm^{-1}$ and 558 $cm^{-1}$ first appear at 0.45 V.

The evolution of the Raman spectrum for Ni oxide deposited on Au can be interpreted in the following manner. For Ni oxide coverages of 1.1 ML, the band observed at 555−583 $cm^{-1}$, depending on applied potential, may be assigned to a mixture of Au oxide and/or mixed NiAu oxide or hydroxide. This interpretation is suggested by the recognition that Ni is miscible with Au and the similarity of the band position to that of both Ni and Au oxide.[20,30,31] The asymmetry of the feature at 0.5 V suggests the presence of more than one species. At an intermediate coverage of 2.8 ML, only a single band at ~552 $cm^{-1}$ is observed at 0.4−0.5 V. This band could belong uniquely to a NiAu oxide. For thicker Ni oxide deposits, the spectrum increasingly resembles that of γ-NiOOH. Thus, we propose that the surface of the electrochemically roughened Au is initially covered by a mixed NiAu oxide, but as the thickness of the Ni oxide increases above a monolayer, the dominant form of the deposit is α-$Ni(OH)_2$, which then oxidizes to γ-NiOOH as the potential is raised. The bands at 460−492 $cm^{-1}$ only appear for thick coverages of Ni hydroxides and can be attributed to α-$Ni(OH)_2$ and possibly other lower oxidation states of Ni oxides, for example, NiO (section S5 in Supporting Information).[32]

The evolution of the Raman spectrum of 2mC of Ni oxide deposited on Pd during a LSV scan (Figure 5f) closely resembles that of Ni α/γ or thick Ni oxide films deposited on an Au electrode (Figures 1c and 5e). The comparable ratio of intensities for the 479 $cm^{-1}$ and 558 $cm^{-1}$ bands observed for these three electrodes suggests that α-$Ni(OH)_2$ does not interact with Pd to form a bimetallic oxide but, instead, oxidizes solely to γ-NiOOH as the applied potential is raised. This conclusion is also supported by the cyclic voltammograms of Ni oxide deposited on Pd, which resemble that of bulk Ni (Figure 4b). These observations explain why the OER activity of α-$Ni(OH)_2$ deposited on Pd is significantly lower than that of α-$Ni(OH)_2$ deposited on Au. In fact, the activity of the former is equivalent to that for bulk γ-NiOOH films.

It is noted that the Ni oxides and hydroxides identified by Raman spectroscopy at the different applied potentials are the majority species present. Amorphous Ni oxides could also be formed during voltammetry scans but not detected spectroscopically because their spectral bandwidths are very broad or the Raman scattering cross-sections for these species are very small.

3.3. Mechanism of Oxygen Evolution. Lyons and Brandon have reviewed the literature dealing with the mechanism of oxygen evolution on Ni electrodes.[7] Most of the available evidence suggests that, in its working state, the surfaces of such electrodes are covered by NiOOH, and hence, $Ni^{III}$ cations are the active centers for OER. Nevertheless, a number of authors have suggested that $Ni^{IV}$ cations formed at high potential serve as the active centers.[11] Reaction sequences based on both $Ni^{III}$ and $Ni^{IV}$ can be used to explain the observed Tafel slopes and reaction order in $OH^-$, ~40 mV and 1.0, respectively.[7] The authors note that, while electrochemical measurements cannot discriminate between these alternatives, the mechanism based on $Ni^{III}$ offers the advantage of being able

to explain the loss in OER activity with time, which is attributed to a progressive increase in the proportions of $Ni^{IV}$ to $Ni^{III}$.[6,7] The in situ Raman observations reported here support the conclusion that the surface of bulk Ni electrodes is covered by a layer of either γ-NiOOH or β-NiOOH, depending on the pretreatment of the electrode, and hence, $Ni^{III}$ cations predominate at the catalyst surface. Our work also shows that Ni β/β is more active for the OER than Ni α/γ.

The results presented in Figure 3 clearly demonstrate that a very thin layer of Ni hydroxide deposited onto Au has a significantly higher OER activity relative to a thick layer of Ni hydroxide formed on bulk Ni or electrodeposited on Au. We are aware of only two other studies in which similar effects of Au on the electrochemical properties of Ni have been reported. Yang et al. have measured the activity of bimetallic AuNi nanoparticles for the electrochemical oxidation of formic acid and observed that the highest activity occurs for a bulk Au/Ni ratio of 85:15; however, no explanation was given for this observation.[33] Of even greater relevance to the present investigation is the work of Casella et al., who have reported that thin layers of Ni oxide (<4 nm thick) deposited on Au are more active than pure Ni oxide for the electrochemical oxidation of glucose in NaOH solution.[34] Ex situ XPS characterization of used electrodes showed evidence for both $Ni^{III}$ and $Ni^{II}$ cations. Whereas the ratio of $Ni^{III}/Ni^{II}$ was ~0.15 for a bulk Ni electrode, this ratio rose to ~0.47 when 1.5 nm of Ni oxide was deposited onto Au, suggesting that Au in some way facilitates the oxidation of $Ni^{II}$ to $Ni^{III}$. Another possible role of Au can be inferred from the work of Chou et al., who have reported that the binding energy of Au in a $Au_{0.101}Ni_{0.899}$ alloy increases relative to that of pure Au by 0.1 ± 0.05 eV, due to a charge transfer of 0.1 e from Ni to each Au atom.[35] One can infer from these results that Au may modify the electronic properties of $Ni^{III}$ cations present in a thin film of NiOOH on its surface by a small transfer of charge to the highly electronegative Au. Such an effect would be similar to that of ligands on the electronic properties of a metal cation in organometallic complexes (see, for example, ref 36). Consistent with this line of reasoning, we note that the activity of Ni hydroxide deposited on Pd is significantly lower than that of Ni hydroxide deposited on Au. Since the Pauling electronegativity of Pd is lower than that of Au, the lower degree of charge transfer to Pd than Au might explain the low activity of Ni hydroxide on the Pd system.[37] An identical effect has also been observed for thin layers of Co oxide deposited on Au versus Pd.[16]

We have also examined whether changes in the ohmic loss (*iR* drop) of the Ni hydroxide/Au electrodes could explain the decrease in electrochemical activity of this system as the thickness of the deposited film increases (Figure 3). As discussed by Trassati and co-workers, the total ohmic loss is due to the electrolyte resistance, the oxide (hydroxide) film resistance, and the resistance at the interface between the substrate (Au or Pd) and the oxide (hydroxide) layer.[38] Since the same thickness of electrolyte was used in all of the experiments discussed here, differences in electrolyte resistance would not explain the observed differences in electrode activity. It is unlikely that the ohmic drop through the Ni hydroxide films deposited on Au affects our results since we used films <20 nm in thickness and made measurements at low currents (~1 mA). For example, assuming the resistivity of a Ni hydroxide film to be similar to that for Ni oxide, $10^{-1}-10^{-5}$ ohm·m, the voltage drop across Ni hydroxide films <20 nm in thickness is estimated to be $<10^{-8}$ V.[39,40] This voltage loss is insignificant.

Trassati et al. have also noted that the oxide resistance and interfacial resistance affect the potential difference ($\Delta E_p$) in the anodic and cathodic pair of peaks in the CV curves of Co oxide.[38] The larger the difference between the $\Delta E_p$s of two systems, the larger is the difference in their ohmic losses. To assess whether interfacial resistance for Ni hydroxide deposited on Au and Pd were distinguishable, we compared the values of $\Delta E_p$ measured for the Au and Pd electrodes coated with 2 mC of α-$Ni(OH)_2$ (section S6 in Supporting Information). The values of $\Delta E_p$ for α-$Ni(OH)_2$ deposited on Au and Pd are 65 and 69 mV, respectively, which shows that ohmic losses at the interface between the NiOOH and Pd or Au substrates are very similar. We conclude, therefore, from the above analyses, that the *iR* drops occurring across the films of oxidized Ni used in the present studies are so small that they do not contribute significantly to the observed differences in catalytic activity.

## 4. CONCLUSIONS

In situ Raman spectroscopy has been used to identify the composition of the oxide layer present on bulk Ni and thin layers of Ni oxide deposited on Au and Pd during the electrochemical evolution of oxygen in 0.1 M KOH. The oxide present during oxygen evolution from an initially polished Ni electrode is γ-NiOOH. Aging of this film by electrochemical cycling produces a β-NiOOH film that is 3-fold more active than γ-NiOOH. We have proposed that the OER active species may not be β-NiOOH, as it was observed to undergo oxidation to an unidentified oxide at potentials below the onset of $O_2$ evolution. The turnover frequency of a submonolayer of nickel oxide deposited on Au is approximately an order of magnitude higher than that of γ-NiOOH and twice that of β-NiOOH. However, a similar film deposited on Pd exhibits an activity closer to that of bulk γ-NiOOH. The exceptionally high activity of submonlayers of Ni oxide deposited on Au is attributed to the interaction of the Ni with highly electronegative Au. Efforts are currently in progress to acquire in situ X-ray absorption spectra at the Ni K-edge on Ni oxide/Au electrodes in order to confirm the oxidation state of the Ni sites present.

## ASSOCIATED CONTENT

### * Supporting Information

Experimental information; electrochemical and Raman spectroscopy data. This material is available free of charge via the Internet at http://pubs.acs.org.

## AUTHOR INFORMATION


### Corresponding Author

*E-mail: bell@cchem.berkeley.edu.


### Notes

favoring by the United States Government or any agency thereof. The views and opinions of the authors expressed herein do not necessarily state or reflect those of the United States Government or any agency thereof.
The authors declare no competing financial interest.

## ACKNOWLEDGMENTS

This material is based upon work performed by the Joint Center for Artificial Photosynthesis, a DOE Energy Innovation Hub, supported through the Office of Science of the U.S. Department of Energy under Award Number DE-SC0004993. We thank James K. Wu (Material Sciences Division, Lawrence Berkeley National Laboratory) for fabricating the metal targets, Eric Granlund (College of Chemistry, University of California, Berkeley) for constructing the electrochemical cell, and Shannon L. Klaus and Mary W. Louie for helpful discussions on the article.

## REFERENCES

(1) Turner, J. A. *Science* 2004, *305*, 972.
(2) Turner, J. A.; Sverdrup, G.; Mann, M. K.; Maness, P. C.; Kroposki, B.; Ghirardi, M.; Evans, R. J.; Blake, D. *Int. J. Energy Res.* 2008, *32*, 379.
(3) Trasatti, S. *Electrochim. Acta* 1984, *29*, 1503.
(4) Hall, D. E. *J. Electrochem. Soc.* 1983, *130*, 317.
(5) Li, X. H.; Walsh, F. C.; Pletcher, D. *Phys. Chem. Chem. Phys.* 2010, *13*, 1162.
(6) Lu, P. W. T.; Srinivasan, S. *J. Electrochem. Soc.* 1978, *125*, 1416.
(7) Lyons, M. E. G.; Brandon, M. P. *Int. J. Electrochem. Sci.* 2008, *3*, 1386.
(8) Cappadonia, M.; Divisek, J.; Vonderheyden, T.; Stimming, U. *Electrochim. Acta* 1994, *39*, 1559.
(9) Beverskog, B.; Puigdomenech, I. *Corros. Sci.* 1997, *39*, 969.
(10) Bode, H.; Dehmelt, K.; Witte, J. *Electrochim. Acta* 1966, *11*, 1079.
(11) Juodkazis, K.; Juodkazyte, J.; Vilkauskaite, R.; Jasulaitiene, V. *J. Solid State Electrochem.* 2008, *12*, 1469.
(12) Oliva, P.; Leonardi, J.; Laurent, J. F.; Delmas, C.; Braconnier, J. J.; Figlarz, M.; Fievet, F.; Deguibert, A. *J. Power Sources* 1982, *8*, 229.
(13) Desilvestro, J.; Corrigan, D. A.; Weaver, M. J. *J. Electrochem. Soc.* 1988, *135*, 885.
(14) Hu, Y. N.; Bae, I. T.; Mo, Y. B.; Antonio, M. R.; Scherson, D. A. *Can. J. Chem.* 1997, *75*, 1721.
(15) Biesinger, M. C.; Payne, B. P.; Lau, L. W. M.; Gerson, A.; Smart, R. S. C. *Surf. Interface Anal.* 2009, *41*, 324.
(16) Yeo, B. S.; Bell, A. T. *J. Am. Chem. Soc.* 2011, *133*, 5587.
(17) Lyons, M. E. G.; Brandon, M. P. *J. Electroanal. Chem.* 2010, *641*, 119.
(18) Concepcion, J. J.; Tsai, M. K.; Muckerman, J. T.; Meyer, T. J. *J. Am. Chem. Soc.* 2010, *132*, 1545.
(19) Delahaye-Vidal, A.; Beaudoin, B.; Sac-Epee, N.; Tekaia-Elhsissen, K.; Audemer, A.; Figlarz, M. *Solid State Ionics* 1996, *84*, 239.
(20) Yeo, B. S.; Klaus, S. L.; Ross, P. N.; Mathies, R. A.; Bell, A. T. *ChemPhysChem* 2010, *11*, 1854.
(21) Desilvestro, J.; Corrigan, D. A.; Weaver, M. J. *J. Phys. Chem.* 1986, *90*, 6408.
(22) Kostecki, R.; McLarnon, F. *J. Electrochem. Soc.* 1997, *144*, 485.
(23) Dechialvo, M. R. G.; Chialvo, A. C. *Electrochim. Acta* 1988, *33*, 825.
(24) Conway, B. E.; Tilak, B. V. *Adv. Catal.* 1992, *38*, 1.
(25) Cornilsen, B. C.; Shan, X. Y.; Loyselle, P. L. *J. Power Sources* 1990, *29*, 453.
(26) Hahn, F.; Beden, B.; Croissant, M. J.; Lamy, C. *Electrochim. Acta* 1986, *31*, 335.
(27) Lo, Y. L.; Hwang, B. J. *Langmuir* 1998, *14*, 944.
(28) Zhang, C. J.; Park, S. M. *J. Electrochem. Soc.* 1989, *136*, 3333.
(29) Desilvestro, J.; Weaver, M. J. *J. Electroanal. Chem.* 1986, *209*, 377.
(30) Srnanek, R.; Hotovy, I.; Malcher, V.; Vincze, A.; McPhail, D.; Littlewood, S. *ASDAM Slovakia* 2000, 303.
(31) Zafeiratos, S.; Kennou, S. *Appl. Surf. Sci.* 2001, *173*, 69.
(32) Cornilsen, B. C.; Karjala, P. J.; Loyselle, P. L. *J. Power Sources* 1988, *22*, 351.
(33) Yang, T.; Zhang, L.; Li, X.; Xia, D. *J Alloy. Compd.* 2010, *492*, 83.
(34) Casella, I. G.; Guascito, M. R.; Sannazzaro, M. G. *J. Electroanal. Chem.* 1999, *462*, 202.
(35) Chou, T. S.; Perlman, M. L.; Watson, R. E. *Phys. Rev. B* 1976, *14*, 3248.
(36) Zakzeski, J.; Behn, A.; Head-Gordon, M.; Bell, A. T. *J. Am. Chem. Soc.* 2009, *131*, 11098.
(37) Alonso, J. A.; Girifalco, L. A. *Phys. Rev. B* 1979, *19*, 3889.
(38) Baronetto, D.; Kodintsev, I. M.; Trasatti, S. *J. Appl. Electrochem.* 1994, *24*, 189.
(39) Sasi, B.; Sankar, S.; Nissamudeen, K. M.; Rajan, G.; Bahna, A. H.; Gopchandran, K. G. *J. Optoelectron. Adv. Mater.* 2008, *10*, 2637.
(40) Chen, H. L.; Lu, Y. M.; Hwang, W. S. *Surf. Coat. Technol.* 2005, *198*, 138.